Available online at www.sciencedirect.com
ScienceDirect
Trans. Nonferrous Met. Soc. China 32(2022) 1589−1597
Transactions of Nonferrous Metals Society of China
www.tnmsc.cn

Preparation and characterization of Mg-doped $CaCu_3Ti_4O_{12}$ thin films

Ming JIANG[1,2], Zhan CHENG[3], Dan ZHAO[3], Lei ZHANG[3], Dong XU[1,2]

1. Key Laboratory of Metallurgical Emission Reduction & Resources Recycling, Ministry of Education, Anhui University of Technology, Ma'anshan 243002, China;
2. School of Materials Science and Engineering, Anhui Polytechnic University, Wuhu 241000, China;
3. China Innovation Academy of Intelligent Equipment (Ningbo) Co., Ltd., Ningbo 315700, China

Received 20 May 2021; accepted 8 March 2022

Abstract: Mg-doped $CaCu_{3-x}Mg_xTi_4O_{12}$ (x=0, 0.05, 0.1, 0.15, 0.2, at.%) thin films were prepared by a modified sol−gel method. A comparative study on the microstructure and electrical properties of Mg-doped $CaCu_3Ti_4O_{12}$ (CCTO) thin films was carried out. The grain sizes of the Mg-doped CCTO thin films were smaller in comparison to the undoped CCTO films. Furthermore, compared to undoped CCTO films, Mg-doped CCTO thin films obtained higher dielectric constant as well as excellent frequency stability. Meanwhile, Mg doping could reduce the dielectric loss of CCTO thin films in the frequency range of 10^4−10^6 Hz. The results showed that the Mg-doped CCTO thin films had the better electrical characteristics compared with the undoped CCTO films. The nonlinear coefficient of Mg-doped CCTO thin films at x=0.15 and x=0.1 was improved to 7.4 and 6.0, respectively.

Key words: dielectric material; $CaCu_3Ti_4O_{12}$; Mg doping; dielectric constant; dielectric loss; varistor properties

1 Introduction

In recent years, electronic ceramics have attracted attention due to their excellent electronic properties [1−3]. They were applied to electronic devices such as miniaturization, intelligent and versatile applications. Several groups work on new materials [4,5] and new procedure [6−8] for better dielectric properties. Among many kinds of electronic ceramics, $CaCu_3Ti_4O_{12}$ (CCTO) materials with a perovskite structure have captured a great deal of attention due to their extraordinary dielectric properties [9,10]. SUBRAMANIAN et al [11,12] reported that CCTO ceramics have not only a high dielectric constant of 10^4 in the wide frequency range (10^2−10^6 Hz) at room temperature but also excellent thermal stability over a wide temperature range (100−400 K). Furthermore, CHUNG et al [13] found that CCTO materials also have an excellent nonlinear characteristic, which could resist or even eliminate the impact of transient overvoltage spikes in microelectronics. These excellent electrical properties make CCTO materials potential candidates in information storage field [14−16].

However, the exact mechanism of dielectric properties is still not clear [17]. Above all, HOMES et al [10] considered that a high dielectric constant is caused by an intrinsic mechanism. According to the intrinsic mechanism, the local dipole moment is closely related to the displacement of the central titanium ion. Secondly, other researchers have proposed an external effect from the double boundary, which is the reversed boundary, and some calcium ion alignment deviations [18−20]. Thirdly, an internal barrier layer capacitance model (IBLC), proposed by SINCLAIR et al [21], is the most acceptable explanation. Furthermore, according to the IBLC model, a high dielectric constant is induced by forming an insulating grain

Corresponding author: Dong XU, Tel: +86-555-2311892, E-mail: frank@shu.edu.cn
DOI: 10.1016/S1003-6326(22)65895-3

boundary in an electric field. However, when the temperature is lowered to 100 K, the dielectric constant of CCTO will be less than 100, and no phase change occurs in this temperature range [12]. In addition, the dielectric loss tangent is the most important parameter that hinders the market application of CCTO [22,23]. According to the particularity of the CCTO microstructure, several methods have been used to reduce the dielectric loss [24−26]. A large number of studies have shown that doping cations at Cu or Ti sites is an effective method to improve the performance of CCTO ceramics by designing interface structure and chemical composition [27−29]. Due to the uniform composition, low crystallization temperature and excellent stoichiometry of the sol−gel method, it has been gradually applied to many different scientific research fields in recent years [14,30,31]. In our recent work [14], pure CCTO and Co-doped CCTO films at Cu sites were successfully prepared by sol−gel method. At room temperature and 1 kHz, after Co doping at Cu site, we synthesized a pure CCCTO05 film with very low dielectric loss tangent (~0.012) [32]. After Co doping, the crystal structure, microstructure, dielectric and nonlinear properties are significantly improved [14].

In recent years, some research groups have reported CCTO doped with Mg at the Cu site, which seems to be an effective method to reduce the dielectric loss tangent of CCTO materials [33]. NI and CHEN [34] reported an enhanced dielectric response in $Ca(Cu_{2.9}Mg_{0.1})Ti_4O_{12}$ ceramics at 1 kHz. However, its dielectric loss tangent was as high as 0.2. NAUTIYAL et al [35] reported an excellent relative dielectric constant (3.5×10^4) and low dielectric loss tangent (<0.06) in samples containing 1% MgO at room temperature up to 100 kHz. SUN et al [36] reported that $CaCu_{2.9}Mg_{0.1}Ti_4O_{12}$ ceramics successfully obtained high dielectric constant (~2.52×10^4) and low dielectric loss tangent (~0.017) at 1 kHz and room temperature after being sintered at 1080 °C for 8 h. Compared with CCTO ceramic, CCTO films are more suitable for miniaturization and integration of electronic devices [37]. Many studies have found that Mg doping has a significant effect on the microstructure and electrical properties of CCTO films [22,33,36]. Therefore, in this study, we focused on Mg-doped CCTO films. The crystal structure is controlled by adjusting the composition of the CCTO to achieve the purpose of improving its electrical properties.

2 Experimental

2.1 CCMTO thin films preparation

$CaCu_{3-x}Mg_xTi_4O_{12}$ (x=0, 0.05, 0.10, 0.15, 0.20, at%) (CCMTO) thin films were prepared by the sol−gel method on single crystal Si substrate. At the preparation stage, the amounts of required raw materials, $Cu(NO_3)_2\cdot3H_2O$, $Ca(CH_3COO)_2\cdot H_2O$, $C_{16}H_{36}O_4Ti$, and $Mg(CH_3COO)_2\cdot4H_2O$, were calculated according to the stoichiometric ratio. All of raw materials were of analytical-grade, from Sinopharm Group. $Cu(NO_3)_2\cdot3H_2O$ was dissolved in an appropriate amount of anhydrous ethanol. The solution was fully stirred till became blue, transparent, and uniform. $Ca(CH_3COO)_2\cdot H_2O$ was dissolved in an appropriate amount of deionized water and fully stirred till the solution became colorless, transparent, and uniform. $C_{16}H_{36}O_4Ti$ was dissolved in a certain amount of anhydrous ethanol, and the clathrate was covered with a plastic wrap to prevent hydrolysis of $C_{16}H_{36}O_4Ti$. The solution was fully stirred for a while to obtain a light yellow, transparent, and homogeneous kinds of solution. After mixing three solutions, glacial acetic acid was added to adjust the solution to blue, transparent, and uniform with pH≈3. The beaker mouth was covered with cling film to prevent hydrolysis of $C_{16}H_{36}O_4Ti$ during mixing. After mixing, the solution was kept still for 24 h at room temperature. Finally, eight-layer films (about 800 nm) were prepared by dip coating. To remove liquid organic compounds, each layer was baked for 5 min at 400 °C. After being electroplated, all thin film samples were annealed for 1 h at 750 °C in a muffle furnace.

2.2 Characterization

The phase composition of the films was detected by X-ray diffractometer (XRD, D8 Advance, Bruker, German). The elemental analysis was conducted by scanning electron microscopy (SEM, JSM−7500F, Japan). For the electrical measurement, a silver paste with a diameter of 5 mm was coated on the back of the films and dried at 600 °C for 10 min. Dielectric properties were measured by an Agilent HP4294A impedance analyzer with bias voltage of 0.5 V applied in the frequency range of 10^2−10^8 Hz at room temperature as well as at 1×10^3 Hz at 300−500 K, and nonlinear

$E-J$ characteristics were measured with a DC source (CJP CJ1001, China) [38−40].

3 Result and discussion

3.1 XRD analysis results

Figure 1 shows XRD patterns of $CaCu_{3-x}Mg_xTi_4O_{12}$ thin films. More Mg doping reduced the lattice size and lowered the lattice constant. Consequently, it shifted the main diffraction peak of CCTO slightly to a higher angle. Due to equal charge but slightly smaller ion radius of Mg^{2+} (0.72 Å) than that of Cu^{2+} (0.73 Å), we presume that Mg^{2+} has successfully substituted Cu^{2+} in the lattice. The second phases of both TiO_2 and CuO were detected in Mg-doped samples caused by the following incomplete reaction:

$$CaTiO_3+3TiO_2+3CuO=CaCu_3Ti_4O \quad (1)$$

It can be found that with more Mg doping content (x), the amounts of CuO phase increased significantly. The results show that the partial excess Mg^{2+} replaced the Cu^{2+} phase and produced CuO phase. And doping does not change the crystal structure of perovskite, which is consistent with our previous conclusion [36].

3.2 SEM analysis results

Particle size distribution (PSD) [41] provided important support in understanding the physical and chemical properties of thin film, as shown in Fig. 2. PSD curves of $CaCu_{3-x}Mg_xTi_4O_{12}$ showed that the grain sizes for five types of $CaCu_{3-x}Mg_xTi_4O_{12}$ thin films were narrowly distributed around 106.2, 65.2, 75.0, 65.9, and 58.2 nm, respectively. This showed a clear trend of grain size decrease due to Mg doping.

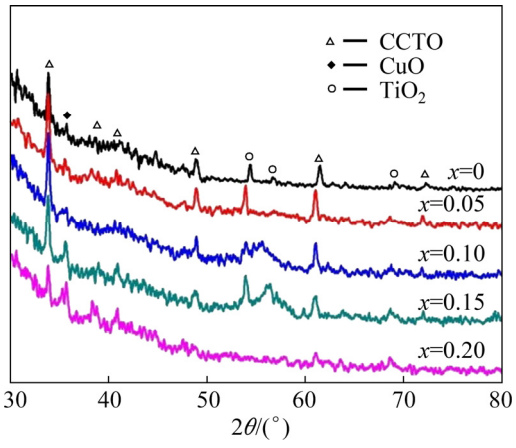

Fig. 1 XRD patterns of $CaCu_{3-x}Mg_xTi_4O_{12}$ thin films

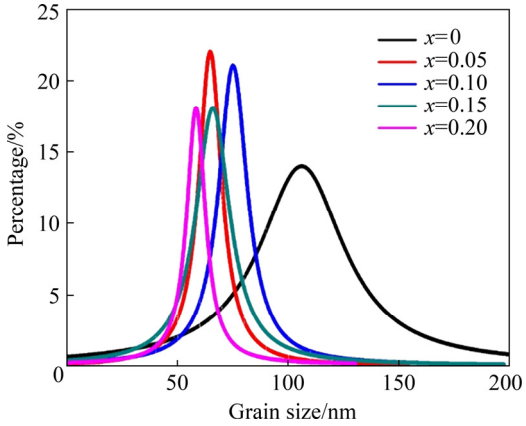

Fig. 2 Particle size distribution of $CaCu_{3-x}Mg_xTi_4O_{12}$ thin films

Furthermore, the surface morphologies of $CaCu_{3-x}Mg_xTi_4O_{12}$ thin films are shown in Fig. 3. From these images, we observed that the grain size in the CCTO thin films decreased with increase of Mg doping content. Simultaneously, number of grain boundaries increased while more gaps came out among grains. PSD was significant for undoped CCTO thin films but not for Mg-doped ones. The reason was that Mg doping produced lots of uniform and smaller grains and wider gaps, which was difficult to be observed. On the other side, Mg doping caused grains of CCTO thin films to tend to be uniform. As seen from Fig. 3, all of these doped thin films were more uniform than the undoped one. Increasing of Mg doping caused grain size smaller and gaps wider, thus decreasing the density. CCTO thin films had comparably higher relative density when x=0.15.

3.3 Dielectric properties

Figure 4 illustrates the influence of Mg doping amount on the real (ε') and imaginary (ε'') parts of the dielectric constant for the CCTO thin film. The ε' for five types of Mg doping samples were 4213, 5143, 5545, 5301, and 4252, respectively, for the measurements at 1 kHz and room temperature. In the frequency range of 10^2−10^4 Hz, the real part ε' first increased and then decreased with the increase of Mg doping content. In all five cases, ε' was the highest when x=0.10 while the lowest when x=0.20, as seen in Fig. 4(a). In the frequency range from 1×10^5 Hz up to 1×10^6 Hz, ε' for Mg-doped CCTO thin film was higher than that for undoped CCTO thin film. With the increase of Mg doping, ε' first increased and then decreased. $CaCu_{3-x}Mg_xTi_4O_{12}$

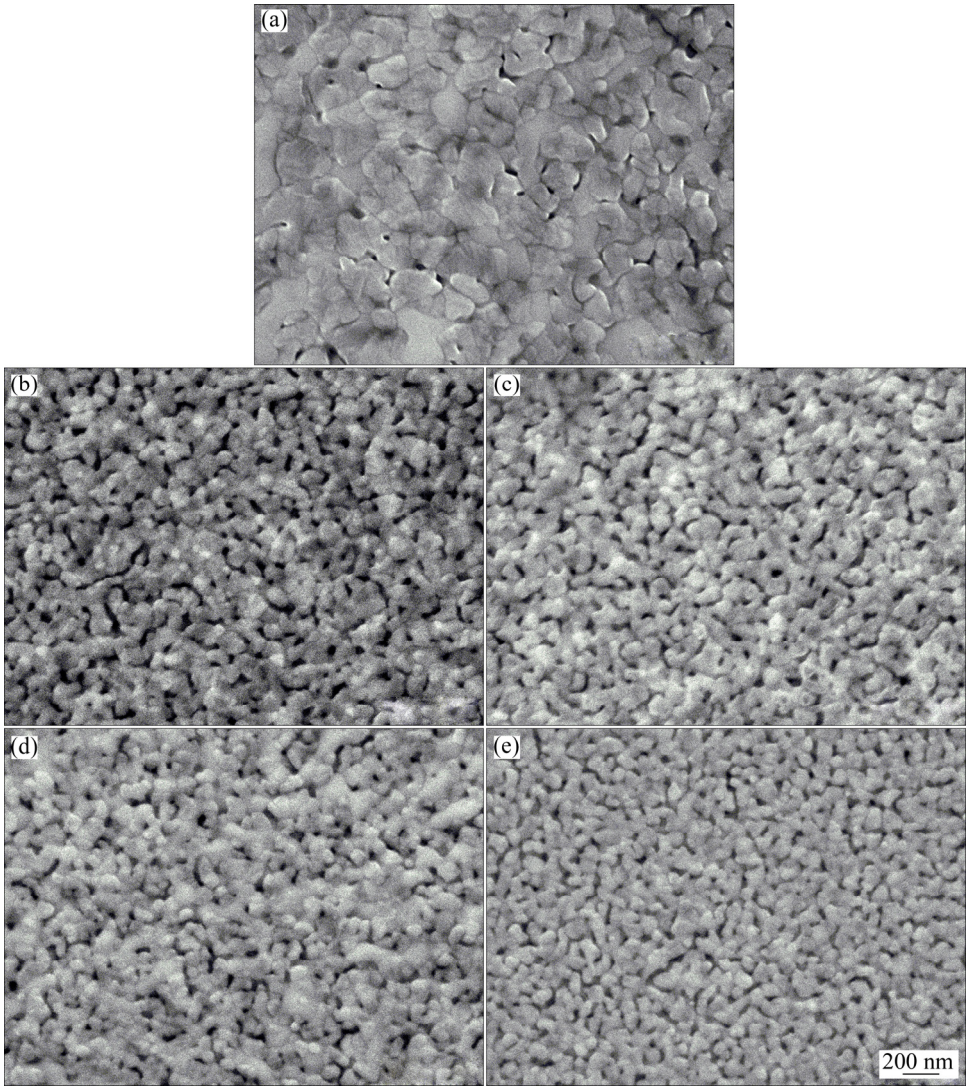

Fig. 3 FE-SEM images of $CaCu_{3-x}Mg_xTi_4O_{12}$ thin films: (a) x=0; (b) x=0.05; (c) x=0.10; (d) x=0.15; (e) x=0.20

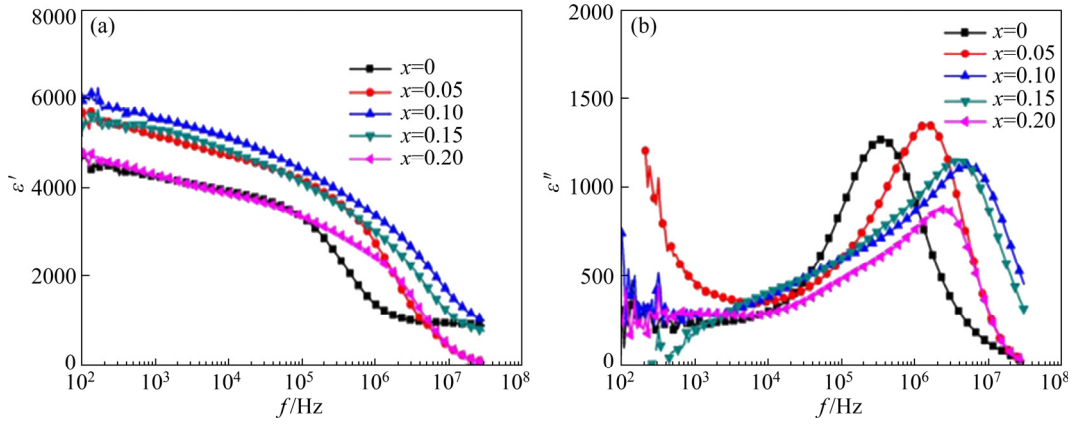

Fig. 4 Frequency dependence of dielectric constant of real (ε') (a) and imaginary (ε'') (b) parts of $CaCu_{3-x}Mg_xTi_4O_{12}$ thin films

thin film when x=0.10 had the highest ε'. In the frequency range of 1×10^6–3×10^7 Hz, ε' suddenly decreased for all doping cases. ε' was higher than that of undoped CCTO when x=0.10 and 0.15. In the whole frequency range, ε' for $CaCu_{3-x}Mg_xTi_4O_{12}$ thin films was always higher than that for the undoped thin film when x=0.10 and 0.15. ε' was the highest when x=0.10. Combined with above

morphological analysis in Fig. 2, grain sizes first increased and then decreased with Mg doping increasing. Average grain sizes of $CaCu_{3-x}Mg_xTi_4O_{12}$ thin film were around 75.0 and 58.2 nm when x=0.10 and 0.20, respectively. Therefore, $CaCu_{3-x}Mg_xTi_4O_{12}$ thin film had the highest dielectric constant ε' when x=0.10. Figure 4(b) illustrates the influence of frequencies on the imaginary parts (ε'') of dielectric constant. Each curve related to each sample had a relaxation peak [41]. With the increase of Mg content in CCTO thin film, relaxation frequency (f_m) first increased and then decreased. The f_m with Mg doping in CCTO thin film was higher than that of undoped CCTO. The f_m for $CaCu_{2.9}Mg_{0.1}Ti_4O_{12}$ (when x=0.1) was the highest. As we notice, the peak frequency was close to the initial fast decreasing frequency of real part (ε') of the dielectric constant. f_m reflects dielectric frequency stability range of thin films. If f_m is higher, then dielectric frequency stability range of thin films is broader. Both $CaCu_{2.9}Mg_{0.1}Ti_4O_{12}$ and $CaCu_{2.85}Mg_{0.15}Ti_4O_{12}$ thin films had wider dielectric frequency stability range. And f_m for $CaCu_{2.9}Mg_{0.1}Ti_4O_{12}$ was the broadest of this range.

Figure 5 illustrates the relationship between dielectric loss tangent (tan δ) and Mg doping of CCTO thin films. It can be obviously seen that dielectric loss tangent (tan δ) was significantly reduced by Mg doping in the frequency range from 1×10^4 up to 1×10^6 Hz. At high frequencies over 1×10^7 Hz, dielectric loss tangent (tan δ) of doped thin film was higher than that of the undoped one. The reason comes from the obvious deviation of dielectric relaxation peak to high frequency due to Mg doping for CCTO thin film. The large increase in the dielectric loss tangent in a low- frequency rage was due to dc conductivity [27,42]. In Fig. 5, f_m corresponding to dielectric loss tangent peak near high frequency region for each sample corresponds to interface relaxation peak frequency of corresponding thin film in Fig. 4(b), and f_m firstly increased and then decreased. When x=0.1, the $CaCu_{2.9}Mg_{0.1}Ti_4O_{12}$ thin film had the highest f_m. At the same time, the dielectric loss tangent for $CaCu_{2.9}Mg_{0.1}Ti_4O_{12}$ thin film was the lowest, which indicates that $CaCu_{2.9}Mg_{0.1}Ti_4O_{12}$ thin film was the most promising one to reduce dielectric loss tangent. According to previous study [43], $CaCu_{2.9}Mg_{0.1}Ti_4O_{12}$ thin film significantly decreased the conductivity of grain boundary layer and enhanced insulating grain boundary. Therefore, $CaCu_{2.9}Mg_{0.1}Ti_4O_{12}$ thin film could significantly decrease dielectric loss tangent.

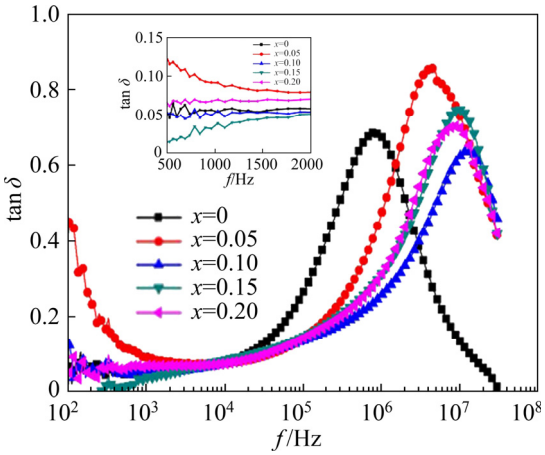

Fig. 5 Frequency dependence of dielectric loss tangent (tan δ) for $CaCu_{3-x}Mg_xTi_4O_{12}$ thin films (The inset is an enlarged view at low frequencies)

The inset of Fig. 5 shows the dielectric loss tangent at room temperature with a change of frequency from 500 to 2000 Hz. At room temperature and 1000 Hz, tan δ values of different Mg doped CCTO thin films were 0.053, 0.091, 0.052, 0.038, and 0.069, respectively.

Figure 6 shows the Cole−Cole plot of $CaCu_{3-x}Mg_xTi_4O_{12}$ thin films. A Cole−Cole circle for each $CaCu_{3-x}Mg_xTi_4O_{12}$ thin film sample was observed. This shows the typical Maxwell−Wagner relaxation mechanism [9,24], that is, the relaxation mechanism produced by inhomogeneous structure composed of internal conductive grain and thin insulating grain boundary at high frequency region. And, typical relaxation peak appeared in each CCMTO sample near high frequency in Figs. 4(b) and 5. $CaCu_{3-x}Mg_xTi_4O_{12}$ thin films had a tail part when x=0.05 and 0.20. This relaxation mechanism was thought to be barrier relaxation mechanism between the electrode and the material in the low-frequency region. This relaxation was more significant for CCMTO thin film when x=0.05 than others and caused high ε' and high dielectric loss tangent. There was no tail part when x=0.10 and 0.15, which could be explained by the IBLC mechanism since microstructures for these two thin film samples were dense as can be seen in Fig. 2. Effect of barrier layer between the electrode and inter-material interface was little, which explained the excellent dielectric property of these two thin film samples.

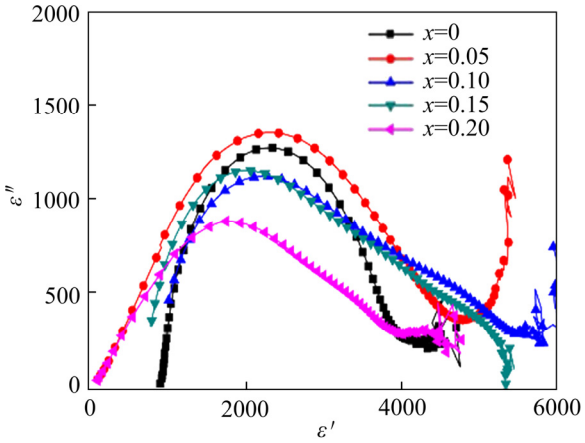

Fig. 6 Cole−Cole plots of $CaCu_{3-x}Mg_xTi_4O_{12}$ thin films

Figure 7 shows dielectric temperature change of different Mg doped CCTO thin films. Figure 7(a) shows the absolute values of dielectric constant thermal stability coefficient ($\Delta\varepsilon'/\varepsilon'$) for CCTO thin films. Form Fig. 7(a) when x=0.05 and 0.20, $\Delta\varepsilon'/\varepsilon'$ was lower than that when x=0.15 in the temperature range of 300−500 K at the frequency of 1 kHz, and temperature range for these two Mg doped CCTO thin films (x=0.05 and 0.20) was close to that of undoped CCTO thin film. When x=0.10 and 0.15, within the temperature range of 300−500 K, the absolute value of dielectric constant thermal stability coefficient of these two CCTO thin films was lower than that when x=0.15. This illustrates suitable doping of Mg could broaden the temperature range of CCMTO thin film application and improve temperature stability.

Figure 7(b) illustrates the influence of Mg doping on dielectric loss tangent of CCTO thin film at different temperatures. It is shown that dielectric loss tangent of all samples increased with temperature increasing. The dielectric loss tangent values for all samples were remarkably increased when the temperature was over 400 K except CCMTO thin film when x=0.10. This increase was not conducive to the application of these thin films.

3.4 Non-ohmic behaviors

Figure 8 shows varistor properties of CCTO thin film with different Mg doping contents [14,22,44]. All E−J curves behaved non-linearly, as seen in Fig. 8(a). In a different coordinate, Fig. 8(b) shows the relation between $E^{1/2}$ and $\ln J$ for $CaCu_{3-x}Mg_xTi_4O_{12}$ thin films, which gave an approximately linear relationship. This linear relation indicates that a typical constant Schottky barriers existed on grain boundaries, which showed that no effect was produced on varistor property of CCTO thin film by Mg doping.

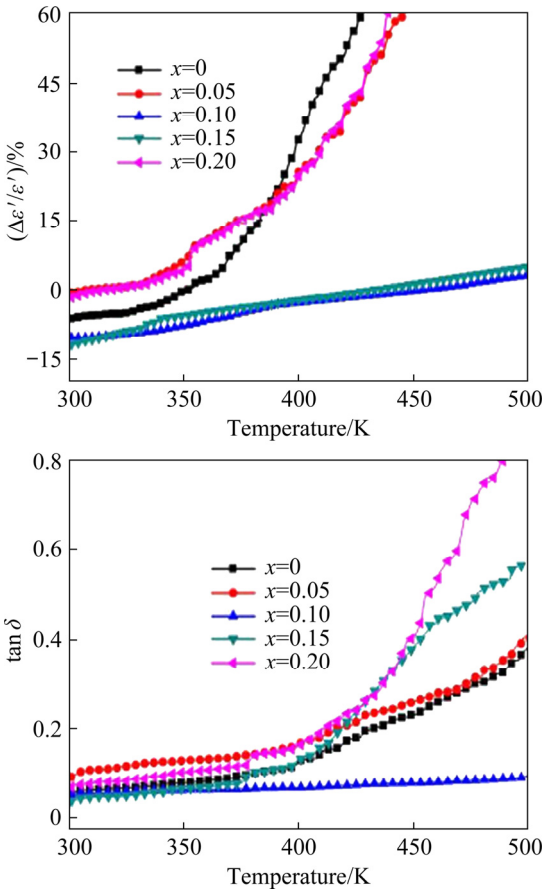

Fig. 7 Effect of temperature on dielectric properties of $CaCu_{3-x}Mg_xTi_4O_{12}$ thin films: (a) Dielectric constant thermal stability coefficient ($\Delta\varepsilon'/\varepsilon'$); (b) Dielectric loss tangent (tan δ)

Table 1 gives the parameters of varistor properties for five types of Mg-doped CCMTO thin films. With more Mg doping content (x), the non-linearity coefficient α first increased and then decreased. When the Cu^{2+} position was replaced by Mg, as a charge compensation, negative defects such as $V_{Cu''}$ occur [45], which changes the structure of the grain boundary, thereby adjusting the height of the barrier and finally affecting the α. But too much Mg doping causes CuO to segregate at the grain boundary and reduces α. When x=0.15, the maximum α reached 7.4. Proper Mg doping could improve varistor property of CCTO thin film. Voltage gradient (V_T) of CCMTO increased with more Mg doping. When x=0.20, voltage gradient (V_T) of CCMTO increased to 45.7 V/mm.

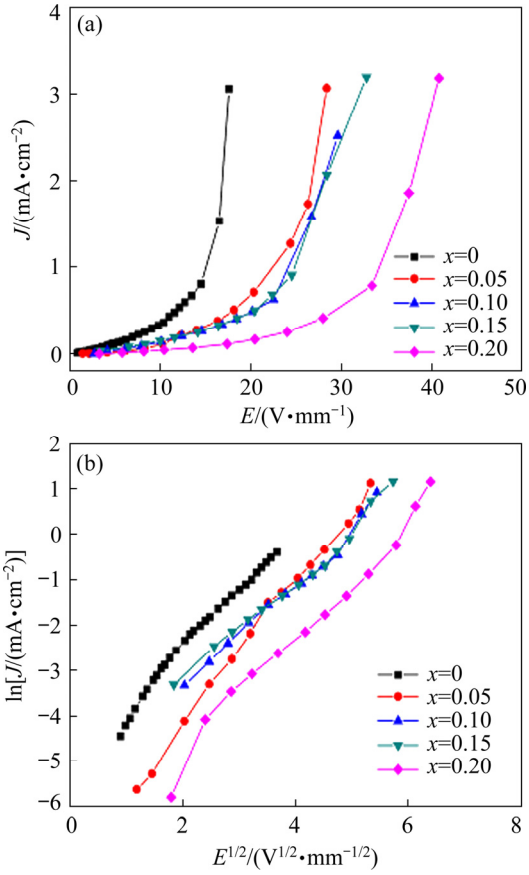

Fig. 8 E–J (a) and $E^{1/2}$–ln J (b) curves of $CaCu_{3-x}Mg_xTi_4O_{12}$ thin films

Table 1 Varistor parameters of Mg-doped CCTO thin films

Sample	α	V_T/(V·mm^{-1})	I_L/μA
x=0	5.3	17.1	141
x=0.05	5.3	26.6	201
x=0.10	6.0	27.7	122
x=0.15	7.4	30.5	109
x=0.20	3.8	45.7	217

We can explain the enhancement through the following relation:

$$V_T=nV_{GB} \quad (2)$$

where n is the number of grain boundaries per unit length and V_{GB} is the average breakdown voltage on grain boundaries. Mg doping reduced the average grain size of the CCTO thin film and increased the number of grain boundaries per unit length, n. Thus, voltage gradient (V_T) of CCMTO thin films increased. CCMTO thin films when x=0.10 and 0.15 demonstrated a lower leakage current (I_L) than the undoped sample. This indicates that proper Mg doping could significantly decrease leakage current (I_L) of CCTO thin films and improve the stability of devices.

4 Conclusions

(1) Microstructure and electrical properties of $CaCu_{3-x}Mg_xTi_4O_{12}$ (x=0, 0.05, 0.1, 0.15, 0.2, at.%) thin films were studied. Part of excess Mg^{2+} replaced the Cu^{2+} species, which led to appearing of CuO phase. Mg doping also decreased grain sizes and caused uniform distribution of grains of CCTO thin films.

(2) In the frequency range from 1×10^4 to 1×10^6 Hz, proper Mg doping could decrease dielectric loss tangent, improve dielectric constant ε' and extend the range of thermal stability. $CaCu_{2.9}Mg_{0.1}Ti_4O_{12}$ thin film significantly decreased the conductivity of grain boundary layer and enhanced insulating grain boundary, and therefore it had the lowest dielectric loss tangent. Also the $CaCu_{2.9}Mg_{0.1}Ti_4O_{12}$ thin film had the best temperature stability.

(3) The Mg doping enhanced the resistivity of insulating grain boundary layer, and the nonlinear coefficient α could reach 7.4 when x=0.15 and as high as 6.0 when x=0.10. Mg doping has potential significance in the property enhancement of thin films and future development of functional devices.

Acknowledgments

The authors are grateful for the financial supports from the National Natural Science Foundation of China (Nos. 52072004, 51802003, 51572113).

References

[1] MU Chun-hong, ZHANG Huai-wu, LIU Ying-li, SONG Yuan-qiang, LIU Peng. Rare earth doped $CaCu_3Ti_4O_{12}$ electronic ceramics for high frequency applications [J]. Journal of Rare Earths, 2010, 28(1): 43−47.

[2] LIU Yang, YU Yang, YIN Chen-yi, ZHENG Liang, ZHENG Peng, BAI Wang-feng, LI Li-li, WEN Fei, ZHANG Yang. Achieving remarkable piezoelectric activity in Sb−Mn co-modified $CaBi_4Ti_4O_{15}$ piezoelectric ceramics [J]. Transactions of Nonferrous Metals Society of China, 2021, 31(8): 2442−2453.

[3] QIU Shen-yu, LI Wang, LIU Yu, LIU Gui-hua, WU Yi-qiang, CHEN Nan. Phase evolution and room temperature ferroelectric and magnetic properties of Fe-doped $BaTiO_3$ ceramics [J]. Transactions of Nonferrous Metals Society of China, 2010, 20(10): 1911−1915.

[4] MONTERO-TAVERA C, DURRUTHY-RODRÍGUEZ M D, CORTÉS-VEGA F D, YAÑEZ-LIMÓN J M. Study of the structural, ferroelectric, dielectric, and pyroelectric properties of the $K_{0.5}Na_{0.5}NbO_3$ system doped with Li^+, La^{3+}, and Ti^{4+} [J]. Journal of Advanced Ceramics, 2020, 9(3): 329−338.

[5] WANG Hao, ZHOU Fu-ming, GUO Jian-ming, ZHANG Yuan-yuan, YANG Hui, ZHANG Qi-long. Surface-modified $Zn_{0.5}Ti_{0.5}NbO_4$ particles filled polytetrafluoroethylene composite with extremely low dielectric loss and stable temperature dependence [J]. Journal of Advanced Ceramics, 2020, 9(6): 726−738.

[6] GROŃ T, MACIEJKOWICZ M, TOMASZEWICZ E, GUZIK M, OBOZ M, SAWICKI B, PAWLUS S, NOWOK A, KUKUŁA Z. Combustion synthesis, structural, magnetic and dielectric properties of Gd^{3+}-doped lead molybdato-tungstates [J]. Journal of Advanced Ceramics, 2020, 9(2): 255−268.

[7] DU Ji-shi, TANG Bing-hua, LIU Wei, ZHANG Tao, PENG Jia-gen, CHEN Hu, LEI Yang-jun. Effects of annealing and firing in wet hydrogen on the dielectric break down strengths of alumina ceramics [J]. Journal of Advanced Ceramics, 2020, 9(2): 173−182.

[8] ZHONG Xin, ZHANG Chen, CHEN Fang-xu, TANG Zhu-ming, JIAN Gang. Dielectric properties and relaxor ferroelectric behavior of $(1–y)Ba(Zr_{0.1}Ti_{0.9})O_3–yBa(Zn_{1/3}Nb_{2/3})O_3$ ceramics [J]. Transactions of Nonferrous Metals Society of China, 2020, 30(3): 756−764.

[9] SUPRIYA D M, RAJANI M R, PHANI A R, NAVEEN C V S, RAVISHANKAR R. Synthesis of CCTO and doped CCTO nanopowders and its applications in the field of electronics [J]. Materials Today: Proceedings, 2017, 4(11): 12021−12025.

[10] HOMES C C, VOGT T, SHAPIRO S M, WAKIMOTO S, RAMIREZ A P. Optical response of high-dielectric-constant perovskite-related oxide [J]. Science, 2001, 293(5530): 673−676.

[11] SUBRAMANIAN M A, SLEIGHT A W. $ACu_3Ti_4O_{12}$ and $ACu_3Ru_4O_{12}$ perovskites: High dielectric constants and valence degeneracy [J]. Solid State Sciences, 2002, 4(3): 347−351.

[12] SUBRAMANIAN M A, LI D, DUAN N, REISNER B A, SLEIGHT A W. High dielectric constant in $ACu_3Ti_4O_{12}$ and $ACu_3Ti_3FeO_{12}$ phases [J]. Journal of Solid State Chemistry, 2000, 151(2): 323−325.

[13] CHUNG S Y, KIM I D, KANG S J. Strong nonlinear current–voltage behaviour in perovskite-derivative calcium copper titanate [J]. Nature Materials, 2004, 3(11): 774−778.

[14] XU Dong, YUE Xian-ning, ZHANG Yu-dong, SONG Juan, CHEN Xiang, ZHONG Su-juan, MA Jia, BA Li, ZHANG Lei, DU San-ming. Enhanced dielectric properties and electrical responses of cobalt-doped $CaCu_3Ti_4O_{12}$ thin films [J]. Journal of Alloys and Compounds, 2019, 773: 853−859.

[15] XU Dong, YUE Xian-ning, SONG Juan, ZHONG Su-juan, MA Jia, BAO Li, ZHANG Lei, DU San-ming. Improved dielectric and non-ohmic properties of (Zn+Zr) codoped $CaCu_3Ti_4O_{12}$ thin films [J]. Ceramics International, 2019, 45(9): 11421−11427.

[16] GRZEBIELUCKA E C, MONTEIRO J F H L, SOUZA E C F D, BORGES C P F, ANDRADE A V C D, CORDONCILLO E, BELTRÁN-MIR H, ANTUNES S R M. Improvement in varistor properties of $CaCu_3Ti_4O_{12}$ ceramics by chromium addition [J]. Journal of Materials Science and Technology, 2019, 41: 12−20

[17] MOUSSA S M, KENNEDY B J. Structural studies of the distorted perovskite $Ca_{0.25}Cu_{0.75}TiO_3$ [J]. Materials Research Bulletin, 2001, 36(13/14): 2525−2529.

[18] BUENO P R, TARARAN R, PARRA R, JOANNI E, RAMÍREZ M A, RIBEIRO W C, LONGO E, VARELA J A . A polaronic stacking fault defect model for $CaCu_3Ti_4O_{12}$ material: An approach for the origin of the huge dielectric constant and semiconducting coexistent features [J]. Journal of Physics D: Applied Physics, 2009, 42(5): 055404.

[19] XU Dong, HE Kai, YU Ren-hong, SUN Xiu-juan, YANG Yong-tao, XU Hong-xing, YUAN Hong-ming, MA Jing. High dielectric permittivity and low dielectric loss in sol–gel derived Zn doped $CaCu_3Ti_4O_{12}$ thin films [J]. Materials Chemistry and Physics, 2015, 153: 229−235.

[20] SINGH L, KIM I W, SIN B C, MANDAL K D, RAI U S, ULLAH A, CHUNG H, LEE Y. Dielectric studies of a nano-crystalline $CaCu_{2.90}Zn_{0.10}Ti_4O_{12}$ electro-ceramic by one pot glycine assisted synthesis from inexpensive TiO_2 for energy storage capacitors [J]. RSC Advances, 2014, 4(95): 52770−52784.

[21] SINCLAIR D C, ADAMS T B, MORRISON F D, WEST A R. $CaCu_3Ti_4O_{12}$: One-step internal barrier layer capacitor [J]. Applied Physics Letters, 2002, 80(12): 2153−2155.

[22] XIAO Mi, LI Lei, ZHANG Ping. Non-Ohmic properties of $MgTiO_3$ doped $CaCu_3Ti_4O_{12}$ thin films deposited by magnetron sputtering method [J]. Journal of Alloys and Compounds, 2018, 743: 570−575.

[23] LIN He, HE Xiang, GONG Yun-yun, PANG Dong-fang, YI Zhi-guo. Tuning the nonlinear current−voltage behavior of $CaCu_3Ti_4O_{12}$ ceramics by spark plasma sintering [J]. Ceramics International, 2018, 44(7): 8650−8655.

[24] ALMEIDA-DIDRY S D, NOMEL M M, AUTRET C, HONSTETTRE C, LUCAS A, PACREAU F, GERVAIS F. Control of grain boundary in alumina doped CCTO showing colossal permittivity by core-shell approach [J]. Journal of the European Ceramic Society, 2018, 38(9): 3182−3187.

[25] JUMPATAM J, CHANLEK N, TAKESADA M, THONGBAI P. Giant dielectric behavior of monovalent cation/anion (Li^+, $F^–$) co-doped $CaCu_3Ti_4O_{12}$ ceramics [J]. Journal of the American Ceramic Society, 2020, 103: 1871−1880.

[26] BOONLAKHORN J, CHANLEK N, MANYAM J, SREPUSHARAWOOT P, THONGBAI P. Simultaneous two-step enhanced permittivity and reduced loss tangent in Mg/Ge-doped $CaCu_3Ti_4O_{12}$ ceramics [J]. Journal of Alloys and Compounds, 2021, 877: 160322.

[27] KAFI Z, KOMPANY A, ARABI H, ZAK A K. The effect of cobalt-doping on microstructure and dielectric properties of $CaCu_3Ti_4O_{12}$ ceramics [J]. Journal of Alloys and Compounds, 2017, 727: 168−176.

[28] WANG Jing, LU Zhen-ya, DENG Teng-fei, ZHONG Cai-fu, CHEN Zhi-wu. Improved dielectric properties in A′-site nickel-doped $CaCu_3Ti_4O_{12}$ ceramics [J]. Journal of the American Ceramic Society, 2017, 100(9): 4021−4032.

[29] WANG Jing, LU Zhen-ya, DENG Teng-fei, ZHONG Cai-fu, CHEN Zhi-wu. Improved dielectric, nonlinear and magnetic properties of cobalt-doped $CaCu_3Ti_4O_{12}$ ceramics [J]. Journal of the European Ceramic Society, 2018, 38(10): 3505−3511.

[30] NEZAMDOUST S, SEIFZADEH D, HABIBI-YANGJEH A.

Nanodiamond incorporated sol−gel coating for corrosion protection of magnesium alloy [J]. Transactions of Nonferrous Metals Society of China, 2020, 30(6): 1535−1549.

[31] PENG Ke, ZHANG Zhi-jian, ZHAO Ze-jun, YANG Chao, TIAN Zhong-liang, LAI Yan-qing. Performance of carbon-coated nano-ZnO prepared by carbonizing gel precursor as anodic material for secondary alkaline Zn batteries [J]. Transactions of Nonferrous Metals Society of China, 2019, 29(10): 2151−2159.

[32] YANG Zhi, ZHANG Yue, LU Zhi-hong, ZHANG Kun, XIONG Rui, SHI Jing. Electrical conduction and dielectric properties of the Rb-doped $CaCu_3Ti_4O_{12}$ [J]. Journal of the American Ceramic Society, 2013, 96(3): 806−811.

[33] JUMPATAM J, MOOLTANG A, PUTASAENG B, KIDKHUNTHOD P, CHANLEK N, THONGBAI P, MAENSIRI S. Effects of Mg^{2+} doping ions on giant dielectric properties and electrical responses of $Na_{1/2}Y_{1/2}Cu_3Ti_4O_{12}$ ceramics [J]. Ceramics International, 2016, 42(14): 16287−16295.

[34] NI L, CHEN X M. Enhanced giant dielectric response in Mg-substituted $CaCu_3Ti_4O_{12}$ ceramics [J]. Solid State Communications, 2009, 149(9/10): 379−383.

[35] NAUTIYAL A, AUTRET C, HONSTETTRE C, ALMEIDA-DIDRY S D, AMRANI M E, ROGER S, NEGULESCU B, RUYTER A. Local analysis of the grain and grain boundary contributions to the bulk dielectric properties of $Ca(Cu_{3-y}Mg_y)Ti_4O_{12}$ ceramics: Importance of the potential barrier at the grain boundary [J]. Journal of the European Ceramic Society, 2016, 36(6): 1391−1398.

[36] SUN Li, ZHANG Ru, WANG Zhen-duo, CAO En-si, ZHANG Yong-jia, JU Lin. Microstructure and enhanced dielectric response in Mg doped $CaCu_3Ti_4O_{12}$ ceramics [J]. Journal of Alloys and Compounds, 2016, 663: 345−350.

[37] PARRA R, SAVU R, RAMAJO L A, PONCE M A, VARELA J A, CASTRO M S, BUENO P R, JOANNI E. Sol–gel synthesis of mesoporous $CaCu_3Ti_4O_{12}$ thin films and their gas sensing response [J]. Journal of Solid State Chemistry, 2010, 183(6): 1209−1214.

[38] XU Dong, CHENG Xiao-nong, ZHAO Guo-ping, YANG Juan, SHI Liyi. Microstructure and electrical properties of Sc_2O_3-doped ZnO–Bi_2O_3-based varistor ceramics [J]. Ceramics International, 2011, 37(3): 701−706.

[39] XU Dong, SHI Li-yi, WU Zhen-hong, ZHONG Qing-dong, WU Xin-xin. Microstructure and electrical properties of ZnO–Bi_2O_3-based varistor ceramics by different sintering processes [J]. Journal of the European Ceramic Society, 2009, 29(9): 1789−1794.

[40] PENG Pai, DENG Yu-jun, NIU Jing-peng, SHI Li-yi, MEI Yun-zhu, DU San-ming, LIU Juan, XU Dong. Fabrication and electrical characteristics of flash-sintered SiO_2-doped ZnO−Bi_2O_3−MnO_2 varistors [J]. Journal of Advanced Ceramics, 2020, 9(6): 683−692.

[41] XU Dong, ZHU Ya-jun, ZHANG Bin, YUE Xian-ning, JIAO Lei, SONG Juan, ZHONG Su-juan, MA Jia, BAO Li ,ZHANG Lei. Excellent dielectric performance and nonlinear electrical behaviors of Zr-doped $CaCu_3Ti_4O_{12}$ thin films [J]. Journal of Materials Science: Materials in Electronics, 2018, 29(6): 5116−5123.

[42] BOONLAKHORN J, SREPUSHARAWOOT P, THONGBAI P. Distinct roles between complex defect clusters and insulating grain boundary on dielectric loss behaviors of (In^{3+}/Ta^{5+}) co-doped $CaCu_3Ti_4O_{12}$ ceramics [J]. Results in Physics, 2020, 16: 102886.

[43] BOONLAKHORN J, KIDKHUNTHOD P, THONGBAI P, MAENSIRI S. Colossal dielectric permittivity and electrical properties of the grain boundary of $Ca_{1-3x/2}Yb_xCu_{3-y}Mg_yTi_4O_{12}$ (x=0.05, y=0.05 and 0.30) [J]. Ceramics International, 2016, 42(7): 8467−8472.

[44] PENG Pai, CHEN Cao-hong, CUI Bing, LI Jia-mao, XU Dong, TANG Bin. Influence of the electric field on flash-sintered (Zr+Ta) co-doped TiO_2 colossal permittivity ceramics [J]. Ceramics International, 2022, 48(5): 6016−6023.

[45] WANG Jing, LU Zhen-ya, DENG Teng-fei, ZHONG Cai-fu, CHEN Zhi-wu. Improved dielectric properties in A0-site nickel-doped $CaCu_3Ti_4O_{12}$ ceramics [J]. Journal of the American Ceramic Society, 2017, 100: 4021−4032.

Mg 掺杂 $CaCu_3Ti_4O_{12}$ 薄膜的制备与表征

姜 明[1,2]，程 战[3]，赵 丹[3]，张 雷[3]，徐 东[1,2]

1. 安徽工业大学 冶金减排与资源循环教育部重点实验室，马鞍山 243002；
2. 安徽工程大学 材料科学与工程学院，芜湖 241000；
3. 中机智能装备创新研究院(宁波)有限公司，宁波 315700

摘 要：采用改进的溶胶凝胶法制备 Mg 掺杂的 $CaCu_{3-x}Mg_xTi_4O_{12}$(x=0、0.05、0.1、0.15 和 0.2，摩尔分数，%)薄膜。对掺 Mg 的 $CaCu_3Ti_4O_{12}$(CCTO)薄膜的微观结构和电性能进行研究。与未掺杂的 CCTO 薄膜相比，掺 Mg 的 CCTO 薄膜的晶粒尺寸较小。此外，与未掺杂的 CCTO 薄膜相比，掺 Mg 的 CCTO 薄膜具有高介电常数和出色的频率稳定性。同时，Mg 掺杂可以减少 CCTO 薄膜在 10^4~10^6 Hz 频率范围内的介电损耗。结果表明，与未掺杂的 CCTO 薄膜相比，掺 Mg 的 CCTO 薄膜具有良好的电学特性，x=0.15 和 x=0.1 的 Mg 掺杂 CCTO 薄膜的非线性系数分别提高到 7.4 和 6.0。

关键词：介电材料；$CaCu_3Ti_4O_{12}$；Mg 掺杂；介电常数；介电损耗；压敏性能

(Edited by Bing YANG)